ISSN: 0974-5823 Vol. 7 No. 2 February, 2022

International Journal of Mechanical Engineering

Synthesis, Characterization of Starch/Urea Blend as Corrosion Inhibitor of Mild Steel in Acidic Media

Ahmed Neamah Thamer[a, b] , Ismaeel M. Alwaan[*c] , Liqaa Hussain Kadhum[a]

[a] Chemistry Department /Collage of Education for Girls/ University of Kufa, Najaf, Iraq.

[b]The General Directorate of Educational in Najaf Al-Ashraf, Dr. Enad Ghazwan Preparatory School, Iraq.

[c]Chemical Engineering Department /College of Engineering/University of Kufa, Najaf, Iraq

Abstract

Organic inhibitors have received a lot of interest as potential inhibitors of corrosion of various metal environments. The corrosion inhibition of mild steel in 1 M of hydrochloric acid was studied using the starch/urea (SU) blend as a biopolymer. Reactions between starch and urea were carried out in the hot melt compression. The weight-loss method was utilized to estimate the efficiency of the new inhibitors on corrosion of mild steel in different temperatures. The FTIR results showed that the O-H and C=O groups were presented in the blend of SU structure. The findings of the weight-loss method showed that the inhibition efficiency (*I*E%) of inhibitor was increased with increase the inhibitor concentration and temperature. The mechanism of chemical adsorption was proposed in this process. The results exhibited that a novel inhibitor of SU obeys the Temkin, Langmuir, and Freundlich adsorption isotherm. The Gibbs free energy, the activation energy, entropy, and enthalpy of adsorption were obtained for the various concentrations of inhibitor (0.2, 0.3, and 0.5 g/L), and the outcomes revealed that the thermodynamic characteristics of a new inhibitor declined with loading of inhibitor. It was concluded that the SU can inhibit mild-steel corrosion by producing compositions with mild steel material.

Keywords: Corn starch; Urea; corrosion; weight loss technique; mild steel; Inhibitor.

1. Introduction

Due to its great mechanical strength, mild steel is one of the most commonly used metals in many industrial operations, including chemical industries, industrial transport, pipeline engineering, steel construction, and others [1]. High corrosion susceptibility in mild steel is a major disadvantage. Mild steel structural components are frequently subjected to corrosive environments, such as those found in industries that use acids for pickling, cleaning, and other processes [2]. In the cleaning, pickling, and acidizing of mining and oil pools, hydrochloric acid and sulfuric acid are used extensively. Furthermore, in several industrial operations, they are often used for removing unwanted scale and rust [3]. The removal of components that allow to decrease corrosion such as temperature modification, air dehumidification, the removal of the dissolved O_2 or solid particles, the control of the pH, or the addition of corrosion inhibitors can provide less aggressive conditions or environment [4].

The use of inhibitors in acidic, alkaline, saline, and other aggressive environments is one of the most convenient practical methods for corrosion protection [5]. The choice of effective inhibitors is based on their electron-donating characteristics and mechanism of action [6]. Organics that have π-bonds and electronegative functional groups are the most efficient inhibitors in their chemical molecular composition. The anti-corrosive characteristics of biomaterials depend mostly upon their power to reach the metal roof that is made up of water molecules replaced at the corrosion interface [7].

In recent years, research has played an important role in developing new and strong organic inhibitors. As a result, the studies have uncovered how electronic and molecular characteristics impact the interchange between an inhibitor molecule and the surface of metal [8]. Organic compounds that have the atoms S, O, and/or N are frequently employed as corrosion inhibitors to prevent the mild steel from corroding in acidic environments. These chemical compositions adsorb on the roof of the metal, blocking the effective locations and thus slowing the corrosion process [9]. Furthermore, numerous Organic compounds containing heteroatoms such as oxygen, sulfur, nitrogen have been reported as efficient corrosion inhibitors for minerals and alloys in commercial aqueous acid to decrease the dissolution of the metallic materials [10]. The inhibition performance of Cassava starch on steel in 1.0 M of hydrochloric acid solution was estimated by different methods, and its adsorption was theoretically studied by both quantum chemical computation and molecular dynamic emulation. The outcomes suggest that Cassava starch gives an optimum inhibition efficiency [11]. M. Mobin et al. investigated the corrosion inhibition of mild steel in 0.1M H_2SO_4 in presence of starch. The results showed that the inhibition efficiency was improved with presence of starch [12]. Urea and its compounds represent an important material to prevent the progression of corrosion of metals and alloys because the N_2 and O_2 atoms in their structures play significant role in this process [13]. The corrosion inhibition of mild steel was studied using urea as an inhibitor. It was observed that the inhibition efficiency (IE) increased by increasing the concentration of urea. It was suggested that the corrosion inhibition mechanism was according to cathodic reactions [14].

The efficiency of corrosion inhibition of natural material compositions is linked to their adsorption properties. Adsorption relies on the kind and status of the metal roof, the species of oxidize medium, and the inhibitor's chemical construction [15]. Moreover, the adsorption is also assumed to rely on the probable interactivity of the inhibitor's π-orbitals with the d-orbitals of the particles roof, which encourages the figuration film of corrosion preservation [16]. The absorption of inhibitors on the mineral surfaces causes the effective positions of the metal roof to be covered, resulting in a reduction in the rate of metal corrosion. Furthermore, the type of metal and its face charge, the chemical structure of organic controllers, and the electron distribution in the molecule all have an impact on inhibitor adsorption operation [17].

Recently, the use of natural material inhibitors as corrosion restraints for various metals environments has attracted attention [9]. In our study, the starch/urea blend (SU) was utilized as a corrosion inhibitor for mild steel in acidic environments. Thus, the purpose of this study is to assess the corrosion inhibitory characteristics of SU. The present study used the weight loss technique to investigate corrosion inhibition for mild steel in 1M HCl solution using the SU blend as a new corrosion inhibitor. Moreover, the temperature influence in the range of 20–50 ∘C on corrosion attitude was investigated in the absence and presence of inhibitors. To the best of our knowledge, there has not been any methodical consideration on the effect of SU blend on the corrosion of mild steel in 1 M HCl solution.

2. Experimental

2.1. Materials.

Mild steel (ST37-2) of Iranian manufacture was obtained from the commercial markets. The length of metal samples was 2.0 × 2.0 × 0.18 cm. These slices were utilized with further burnish for the exposed flat surface with different grade emery papers (in the range of 180 - 1200). The specimens were cleaned from grease using distilled water, absolute ethanol and were dried in acetone, and then the specimens were kept in desiccators to avoid the humidity effect until they were utilized in the study of corrosion. The chemical composition of steel alloy is shown in Table (1). The results of chemical composition were obtained by German-made Spectro Max device. The starch was obtained as manufactured by Meptico-Lebanon; the urea from Thomas Backer (chemicals), a manufacturing and marketing company based in Mumbai-India; HCl acid (35-38%) with density (1.18), M.Wt (36,46 g/mol) was obtained from SD Fine-Chem Limited Mumbai-India; and H_2SO_4 acid (96%) with density (1.84), M.Wt. (98.08 g/mol) was received from Belgium. Tetra-methyl-thiuram disulfide (TMTD), zinc oxide and fatty acid (stearic acid) has been used as a catalyst from the Sober companies, India. The stock solution of HCl at the concentration of 1M was attended by mitigation of 37% weight of concentrated hydrochloric acid utilizing bi-distilled water.

Table 1: The mild steel alloy compositions (wt.%)

Element	C%	Si%	Mn%	P%	S%	Cr%	Mo%	Ni%	Cu%	Al%	Fe%
Wt%	0.0664	0.0042	0.367	0.0097	0.0077	0.0063	<0.002	0.0325	0.0049	0.0408	BaL

2.3. Preparation of inhibitor

The blend was prepared with a starch to urea proportion of 60:40 wt.%. Starch:Urea, zinc oxide (ZnO), stearic acid and TMTD were premixed in the electrical mixer, as shown in Table 2, until a homogeneous blend was obtained. The reaction of corn starch with urea and other motivating factors such as tetra-methyl-thiuram disulfide (TMTD), zinc oxide and fatty acid (stearic acid) used as a catalyst in the cross-linking reaction between starch and urea was carried out. The mixtures were processed in a compression molding (Moore, England) at temperature of 165℃, at pressure of 4 Mpa and at time period of 15 min. At the end of the reaction period, the mixture was washed well with abundant distilled water to remove the remaining unreacted urea, and then it was washed using dilute acid from HCl, as well as ethanol: water mixture (70:30), and finally with pure ethanol for the purpose of drying them. The extent of the reaction is expressed in the following equations [18],[19]:

Table 2: Starch / Urea and additives blends in phr.

Materials	Starch (wt%)	Urea (wt%)	ZnO[a]	Stearic acid[a]	TMTD [a,b]
Formulation	60	40	3	2	3

a = phr from total of Starch/ Urea blend; b = Tetramethyl thiuram disulfide .

$$St - OH + CO(NH_2)_2 \xrightarrow{heat} St - OCONH_2 + NH_3 \quad \ldots\ldots\ldots\ldots (1)$$

$$2St - OCONH_2 \xrightarrow{heat} St - OCONHCOO - St + NH_3 \quad \ldots\ldots\ldots\ldots (2)$$

$$St - OH + St - OCONH_2 \xrightarrow{heat} St - OCOOSt + NH_3 \ldots\ldots\ldots (3)$$

Where $St - OH$ is starch.

2.4. Weight Loss Method

Coupons with 2.0 × 2.0 × 0.18 cm dimension have been cleaned and weighed. The samples were held in the middle of the corrosive media which contain 100ml of 1M hydrochloric acid with and without different concentrations of inhibitor. The samples were placed in a vibrator water bath at a temperature range of 20 - 50 ℃ for specific time at interval of 2-5 hours. When the treated time was finished, the samples were scrubbed utilizing a soft bristle brush under current water so as to remove the corrosion output. The samples were then, dried and reweighed.

The variation in the weight of the samples between initial weight and weight at a specific period of time was taken to be weight loss. The calculations were achieved by Sartorius Entris TE64 electronic balance with a sensibility ±0.0001g at the factory in Germany. The outcomes rely on the average of three assessments, and the average amount of the weight lack is fixed. The corrosion rate of mild steel has been estimated for a five-hour inundation period with and without different concentrations of the inhibitor. The corrosion rate were determined according to following equation [20]:

$$CR(\mathrm{mg.cm^{-2}.h^{-1}})r = \frac{\Delta w}{A.t} \quad \ldots\ldots\ldots\ldots\ldots\ldots \quad (4)$$

where ΔW is the weight loss (mg), while A, is the areas of an exposed surface of the sample (cm^2) and t represents the exposure time (h).

The percentage and efficiency of inhibition (IE %) was calculated according to equation (5), stated as follows [21]:

$$IE\% = \frac{W_o - Wi}{W_o} \times 100 \quad \ldots\ldots\ldots\ldots\ldots\ldots . (5)$$

where W_o is the value of weight loss in the absence of inhibitor, and Wi is the value of weight loss in the presence of inhibitor.

Evaluation of surface coverage (θ)

$$\text{surface coverage } (\theta) = \frac{W_o - Wi}{W_o} \ldots\ldots\ldots\ldots\ldots (6)$$

where W_o and Wi are the weight reduction per unit time with presence and absence of restraint, respectively. According to this, the relationship between θ and Log C was examined to determine whether or not the inhibitor adsorption followed Temkin's isotherm by obtaining a linear relationship.

2.5. The Fourier Transform Infrared (FTIR) Spectroscopy

Fourier transforms infrared (FTIR) spectroscopy was utilized to study the chemical structure of starch, urea, and starch/urea blend (SU). FTIR specimen was investigated utilizing an Alpha-Bruker (Germany) infrared spectrophotometer. The computation scope was 400-4000 cm^{-1} at aerial temperature, while the accuracy was kept at 16 cm^{-1}.

3. Results and Discussion

3.1. Fourier Transform Infrared (FTIR) Spectroscopy

The FTIR spectrum of native starch as a natural polymer was shown in Figure 1. The FTIR spectrum shows the absorption peaks at the bands of 1146, 2922, and 3285 cm^{-1}. The stretching vibrations of the hydroxide group (O–H) register a band at 3285 cm^{-1}, whereas the stretching vibrations of C-H group appeared at 2922 cm^{-1} band. On the other hand, the presence of the (C–O–C) was confirmed by the peak at 1146 cm^{-1} [22]. The FTIR spectrum of pure urea was shown in Figure 2. The peaks at 3329 and 3427 cm^{-1} were assigned to amide group (N–H) stretching of urea while the peaks at 1597 cm^{-1} was assigned to amide group (N–H) bending vibrations of urea [23]. The stretching vibrations of the carbonyl group (C=O) was shown at a peak of 1675 cm^{-1}. The peak at 1453 cm^{-1} represents the C – N group stretching vibration [13]. Figure 3 illustrates the FTIR spectrum of the starch/urea blend (SU). The peak at (1675 cm^{-1}) was due to the stretching vibrations of carbonyl group (C=O). Also, the stretching vibrations for (C-H) group appeared at 2918 cm^{-1} while the peak at 3327 cm^{-1} was due to the stretching vibration of -OH group. Moreover, some changes were observed in the locations of the peaks in the new SU blend as compared with pure materials, where the stretching vibration peak of -OH group in the SU blend was shifted to 3327 cm^{-1}. In addition, the C–N stretching vibrations at peak 1453 cm^{-1}, amide group (N–H) stretching and bending vibrations at peaks 3329 - 3427 cm−1, and at 1597 cm^{-1}, respectively, was disappeared from FTIR results of SU blend, as shown in Figure 3. The disappearance of C-N, N-H stretching and bending vibrations groups from SU new blend and present C=O group in SU new blend indicated that the reaction between urea and starch occurred

.

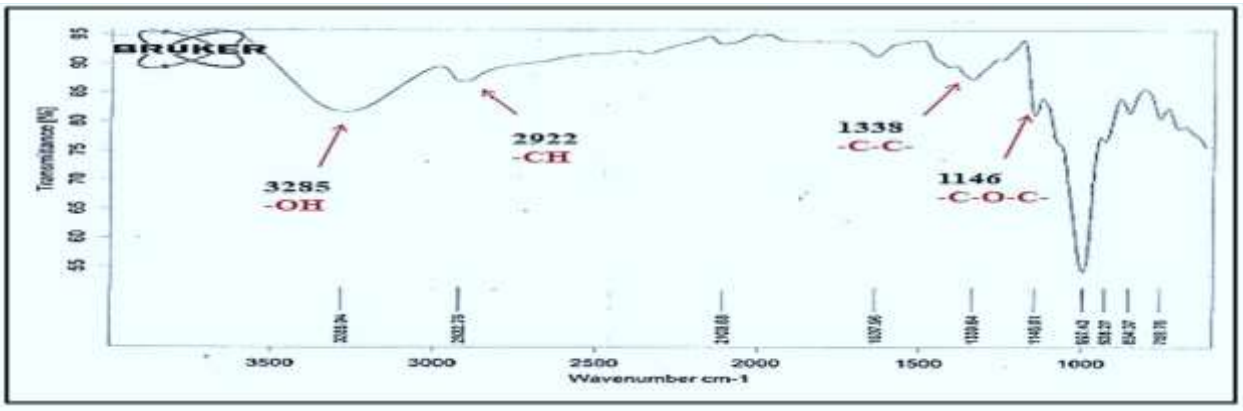

Figure 1: FTIR spectra of starch

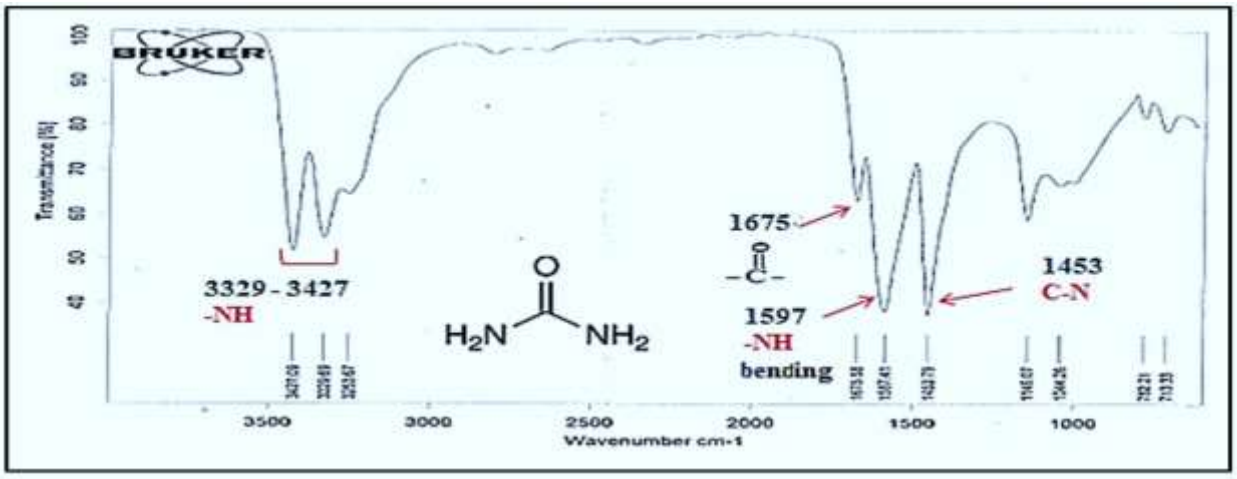

Figure 2: FTIR spectra of urea

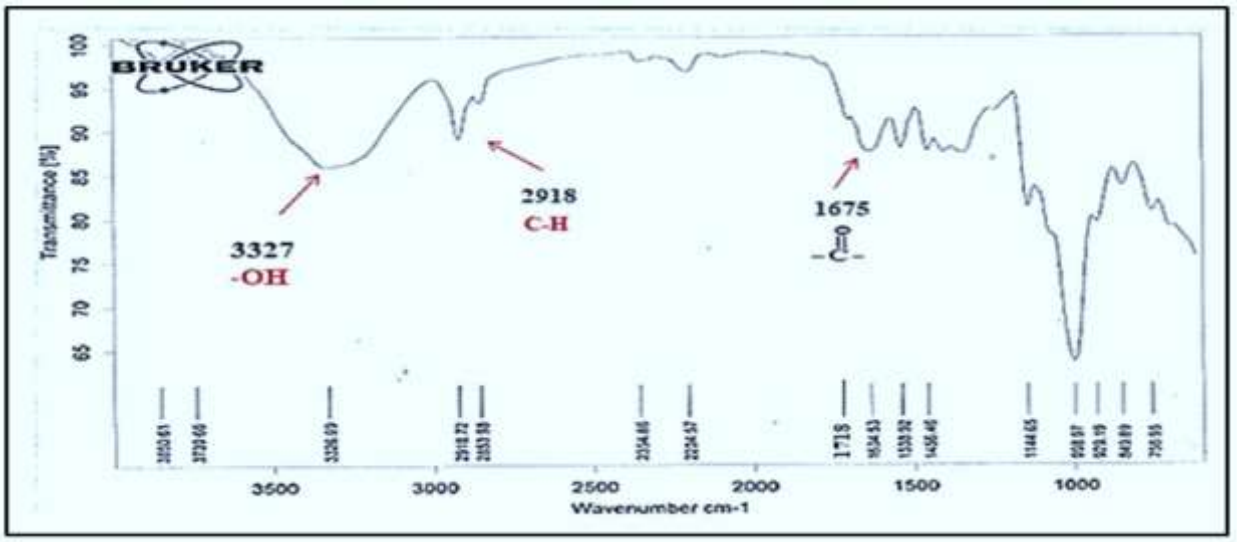

Figure 3: FTIR spectra of SU

3.2. Measurements of Weight Loss

The corrosion of mild steel in 1M HCl with and without SU blend as a restraint of corrosion was studied using the weight loss technique over a temperature range of 20–50ºC. Figure 4 illustrates the relationship of metal weight loss versus time (hours) in 1M hydrochloric acid without and with an inhibitor (0.2, 0.3, and 0.5 g/L) at temperatures of 20, 30, 40, and 50ºC. Weight loss of mild steel with presence of the restraint in the HCl solution was reduced as contrasted to the restraint-free solution, as displayed in Figure 4. The inhibition efficiency and corrosion rates were calculated at the different concentrations of inhibitors and at different temperatures as displayed in Table 3. The results showed that the corrosion rate (*CR*) was reduced in the presence of the SU blend inhibitor as contrasted to the situation of absence of loading of the SU inhibitor in solution. In addition, the corrosion rate increases with temperature increase, indicating that the temperature is a significant operator in the dissolubility of substances [24].

In addition, Maximum inhibitor efficiency was 49% at concentration of 0.5 g/l of inhibitor and at temperature of 50℃, while the minimum value was 18.6 % at concentration of 0.2 g/l of inhibitor and at temperature of 20℃.

Table 3: Corrosion rate (*CR*), inhibition efficiency (*Æ*%), and surface coverage (θ) of mild steel in 1 M HCl for different inhibitor concentrations at different temperatures.

System/ Conc. Wt. g/l	C_R (mg cm^{-2} h^{-1})				Efficiency of Inhibitor (IE%)				Degree of surface coverage (θ)			
	Temperature ºC											
	20℃	30℃	40℃	50℃	20℃	30℃	40℃	50℃	20℃	30℃	40℃	50℃
Blank	0.670	1.190	1.455	2.490	_	_	_	_	_	_	_	_
0.2 g/l	0.545	0.942	1.132	1.850	18.6	20.8	22.2	25.7	0.186	0.208	0.222	0.257
0. 3 g/l	0.480	0.820	0.975	1.605	28.3	31.0	33.0	35.5	0.283	0.31	0.330	0.355
0.5 g/l	0.422	0.690	0.800	1.270	36.9	42.0	45.0	49.0	0.369	0.42	0.45	0.49

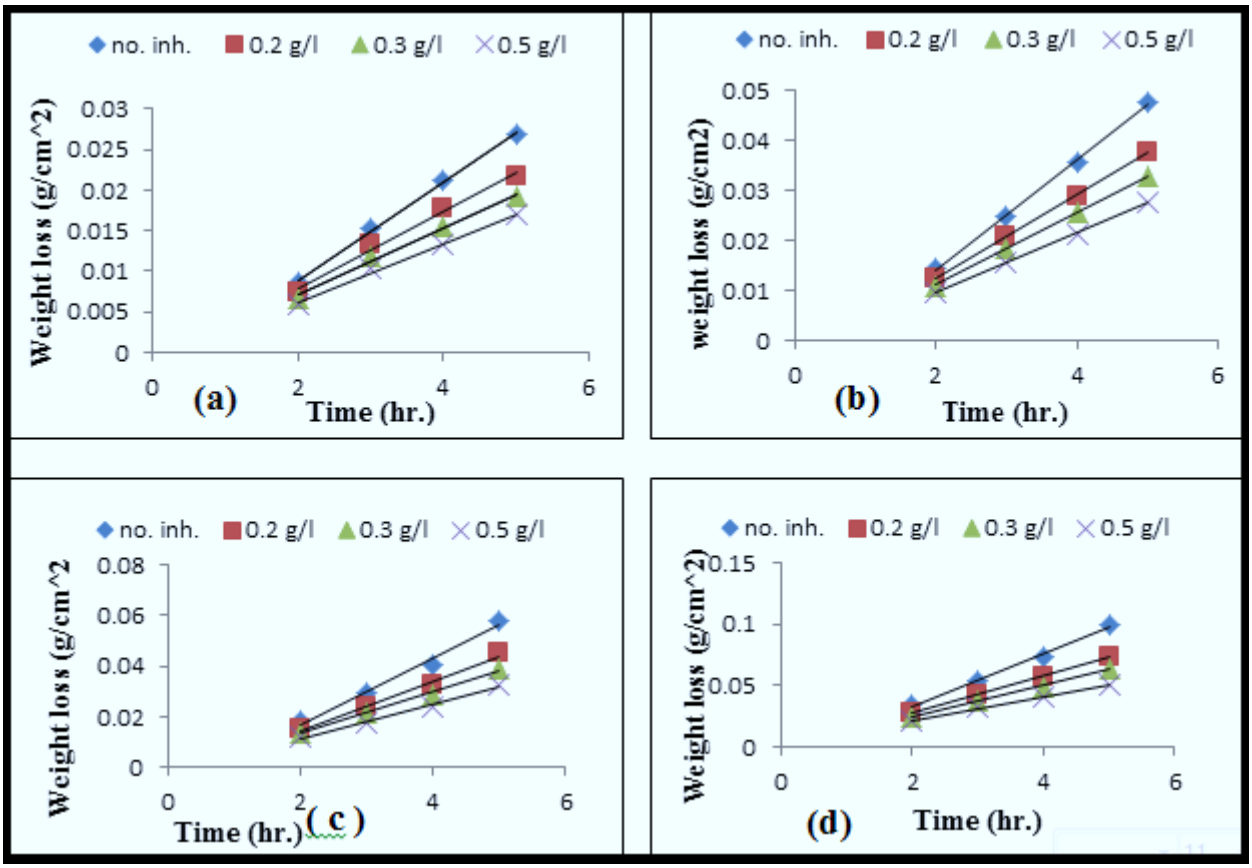

Figure 4: Weight loss of mild steel against time (hours) in 1 M HCl with and without of SU blend at (a) 20∘C, (b) 30∘C, (c) 40∘C, and (d) 50∘C

The adsorption of SU blend on the surfaces of mild steel leads to covering of the mild steel surfaces, which leads to the suppression of corrosion of the mild steel and leads to decrease the corrosion rate. The SU blend has a complicated structure (complex polysaccharide), and the FTIR study showed that SU contains hydroxyl and carbonyl (C=O) groups that tend to adsorb on the face of metal surfaces through the electronic pair on the Oxygen atoms. These polar blends aid in the absorption of SU on the surface of mild steel, which prevent the corrosion operation from occurring. It can be suggested that the SU can prevent mild-steel corrosion by producing components with mild steel material.

3.3. Adsorption Isotherm

Chemical and physical adsorption are the two major kinds of organic compounds adsorption on metal surfaces, and are dependent on the quality of the electronic structure of the metal, the inhibitor compositions, and the media. Figure 5 shows the outcomes of the relevance between the inhibitor concentration (*C*) of SU and the inhibition efficiency (*Æ*%) at different temperatures. The

consequence of suppression efficiency showed that it increases as both the restraint concentration and the temperature rises. With increasing inhibitor concentration and temperature, the inhibition efficacy increases, suggesting that the adsorption operation follows the mechanism of chemical adsorption [25].

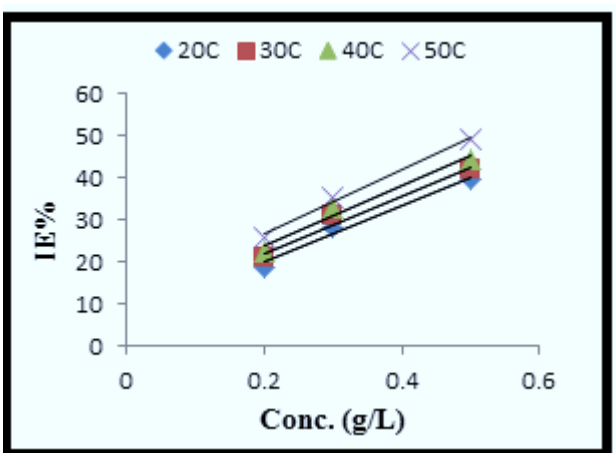

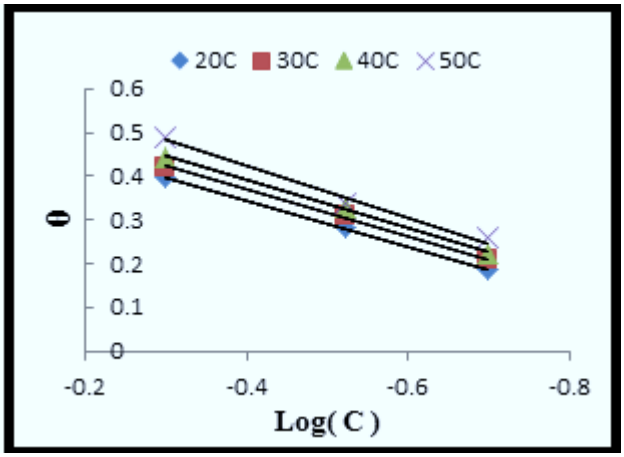

Fig.5: Inhibition efficiency (IE%)of SU versus inhibitor concentration at different.,**Fig.6:**The surface coverage (θ) versus the log(C) of SU at different temperatures.

The surface coverage (θ) values clarified the behavior of adsorption of SU. The following equation can be used to estimate the surface coverage:

$$\theta = \frac{IE\%}{100} \qquad \ldots\ldots\ldots\ldots(7)$$

The surface coverage (θ) values of the inhibitor were used to demonstrate the optimal isotherm for determining adsorption behavior.

The effectiveness of the SU blend as a good inhibitor of corrosion in HCl acid environments depends mainly on its adsorption ability upon the metal surface to understand the mechanism of the SU blend interaction with mild steel in the corrosive media. Langmuir, Frumkin, Temkin, Flory-Huggin, and Freundlich's adsorption isotherms tend to be the better descriptors to match to (θ). To determine the optimal isotherm, the correlation coefficient R^2 was used in comparison with all these models. The best match of (θ) was found using Temkin adsorption isotherms. The equation of the Temkin adsorption isotherm [3, 26] is:

$$Exp\,(-2a\theta) = KC, \ldots\ldots\ldots(7)$$

where "a" is the heterogeneous factor of the metal surface that describes the molecular interactions in the adsorption layer and is referred to as the lateral interaction parameter, and K is the adsorption process equilibrium constant. Figure 6 shows the surface coverage vs the logarithm of SU inhibitor concentration at various temperatures (20, 30, 40, and 50 °C). It is also clear from Figure 6 that the empirical information follows the Temkin adsorption isotherm, as shown by the linear relevance between surface coverage and the SU inhibitor concentration at all temperature ranges. Table 4 shows the adsorption variables of Temkin adsorption isotherms of mild steel corrosion in HCl (1 M) in the presence of SU at 20, 30, 40 and 50 °C.

Table 4: Temkin isotherm parameters at 20, 30, 40, and 50 °C for mild steel in 1M of HCl with SU.

System/ concentration	*a*	*K*	R^2
20°C	− 0.949	2.867	0.9995
30°C	−0.942	2.982	0.9980
40°C	−0.895	2,997	0.9977
50°C	−0.847	3.040	0.9851

The plus and minus signs of the molecular interaction parameter amount (a) can be used to deduce the attraction and repulsion forces between adsorbed molecules, respectively[27]. As shown in Table 3, a repulsion between the adsorbed molecules occurred because the values of "a" were negative [28].The intensity between the adsorbate and the adsorbent is indicated by K. Increased K

values resulted in more efficient adsorption, which leads to better inhibitory efficiency [29]. Chemical adsorption may occur onto the metal surface as a result of increasing *K* values with increase in temperature [3].

3.4. Effect of Temperature

The corrosion of mild steel in HCl (1M) was studied at temperatures ranging from 20 to 50 ° C. with the presence and absence of an SU inhibitor. The results of the plotting logarithm of *CR* vs different temperatures inverse were displayed in Figure 7 for blank and SU inhibitor.

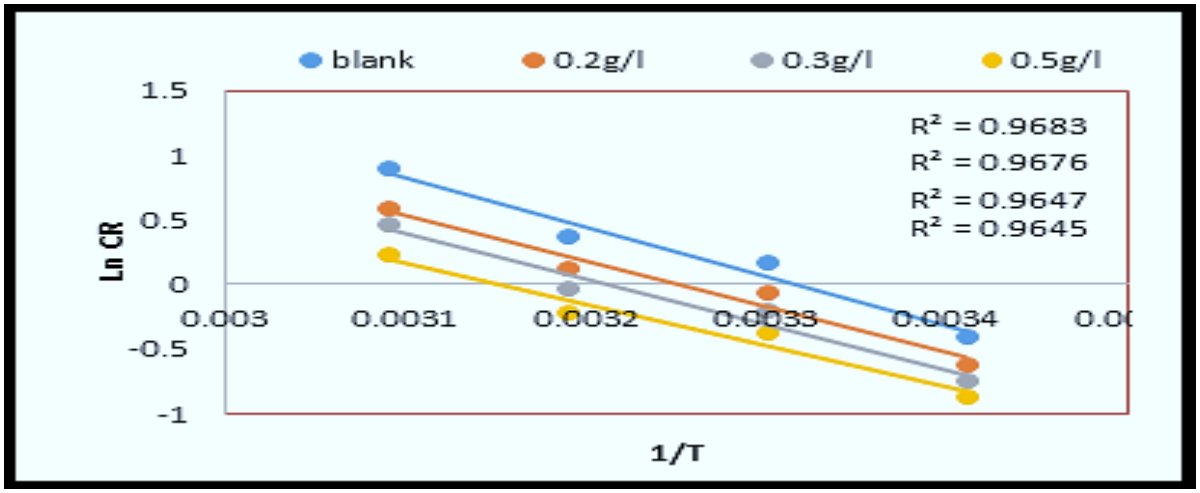

Figure 7: Logarithm of corrosion rate (*CR*) against inverse temperature for mild steel with and without SU in 1M of HCl.

The straight lines were drawn to show that the relationship between the *CR* and temperature follows the Arrhenius equation and that the straight-line slope indicates activation energy.The Arrhenius equation can be written as follows [30]:

$$Ln\ CR = Ln\ A - \frac{\mathrm{Ea}}{\mathrm{RT}} \quad , \ldots\ldots\ldots\ldots (8)$$

The corrosion rate, activation energy, Arrhenius constant, absolute temperature, and molar gas constant are represented as *CR*, *Ea*, *A*, *T*, and *R*, respectively. The activation energy (*Ea*) values are listed in Table 5. The activation energy of the blank sample has more value as compared to the sample with inhibitor loading. It could be attributed to a perceptible increase in inhibitor adsorption on the metal layer as the temperature rises (chemisorption).

Table 5: The activation energy (KJ.mol^{-1}), enthalpy (KJ.mol^{-1}), and entropy (J.mol^{-1}·K^{-1}) of mild steel corrosion in 1M HCl with SU inhibitor.

System/ concentration	Ea (KJ.mol^{-1})	ΔH^o_{ads}(KJ.mol^{-1})	ΔS^o_{ads}(J.mol^{-1}·K^{-1})
Blank	32.090	29.458	−148.988
0.2 g/L	29.550	27.039	−158.912
0.3 g/L	29.425	26.893	−160.511
0.5 g/L	26.861	24.271	−170.545

The enthalpy of adsorption, ΔH, and the entropy of adsorption, ΔS, for mild steel corrosion in 1M HCl with SU inhibitor was calculated using the transition state equation given by [31]:

$$CR = \frac{RT}{Nh}\ exp\left(\frac{\Delta S}{R}\right)\ exp\left(-\frac{\Delta H}{RT}\right), \ldots\ldots\ldots (9)$$

Avogadro's number, molar gas constant, Planck's constant, and absolute temperature are represented as N, R, h, and T, respectively. Figure 8 shows a graph between the logarithm of (CR/T) vs. inverse temperature with the presence and absence of inhibitor. Adsorption enthalpy and adsorption entropy were obtained by slope of ($-\Delta H/R$) and the intersection of the lines, respectively, and the results are presented in Table 5 for various concentrations of inhibitor (0, 0.2, 0.3, and 0.5 g/l). The results suggest that, compared to a blank solution, adsorption enthalpy decreases with the inhibitor loading which confirms the

chemisorption mechanism suggestion. Adsorption entropy has been observed to have negative values, with and without an inhibitor. The negative values indicate that the system order increases [32].

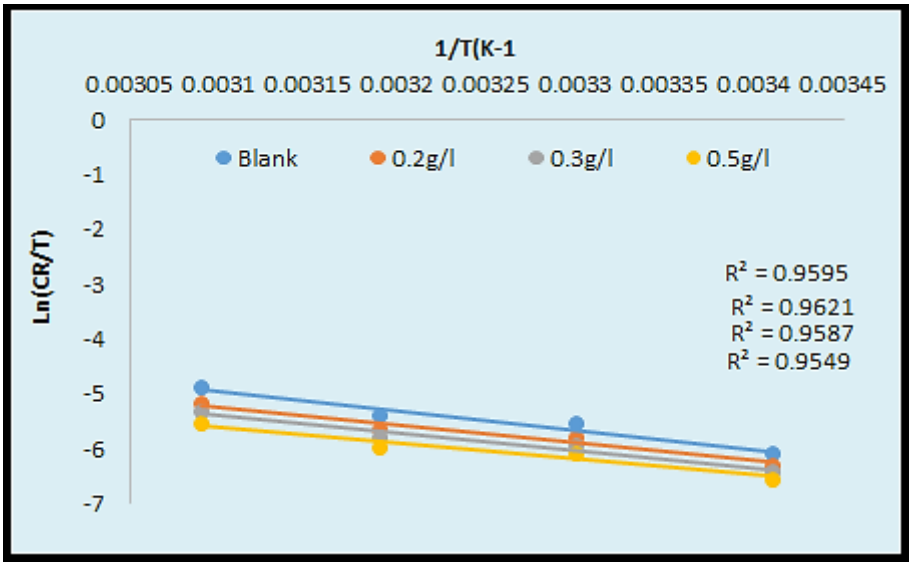

Figure 8: Transition state plot of the corrosion rate for mild steel in 1M HCl with and without SU.

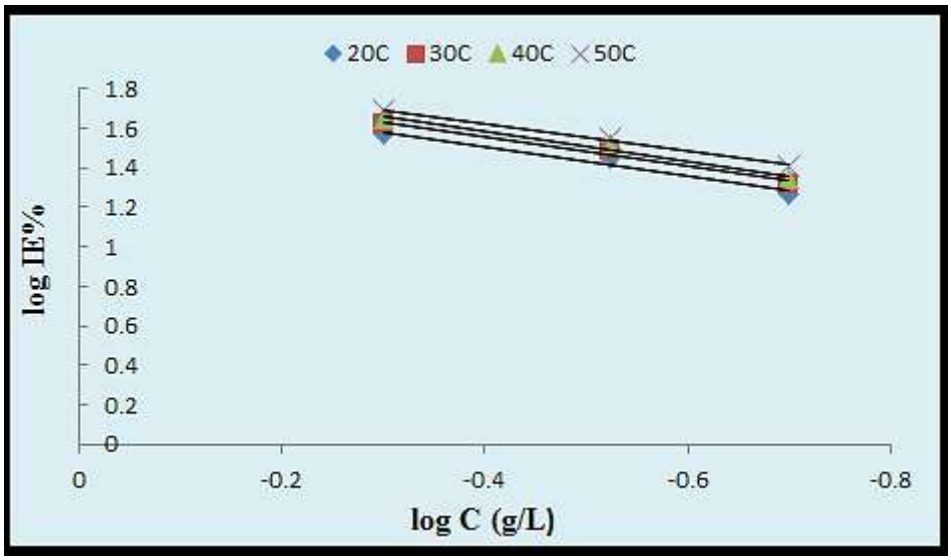

Figure 9: log IE% versus log$C$ for mild steel corrosion in 1M HCl for SU at 20, 30, 40, and 50°C.

The interception of a track line got from the log IE% vs log C graph gives the free energy of adsorption (ΔG^{o}_{ads}) as shown in Figure 9 according to the equation below [33]:

$$\log \mathrm{C} = \log\frac{\theta}{1-\theta} - \log B \,, \ldots\ldots\ldots\ldots\ldots (10)$$

Where

$$\log B = -1.47 - \left(\frac{\Delta G^{\circ}_{ads}}{2.303RT}\right), \ldots\ldots\ldots\ldots (11)$$

Table 6 shows the negative results of free adsorption energy (ΔG^{o}_{ads}) at temperature (20, 30, 40 and 50°), which indicates that SU inhibitor is spontaneously adsorbed.

Table 6: Gibbs free energy of mild steel corrosion in 1M HCl with SU.

Temperature (∘C)	ΔG^{o}_{ads} (KJ.mol^{-1})
20	−19.884
30	−20.732
40	−21.777
50	−22.546

4. **Mechanism of Corrosion Inhibition**

The efficiency of the SU blend to act as a corrosion inhibitor depends on its ability to adsorb on the metal surface. The inhibition efficiency of organic matter is mostly related to its adsorption on the metal surface at constant temperatures [34]. It is well recognized that the adsorption of an restraint always represents a supplanting reaction, which involves removing of H_2O molecules to adsorb on the metal roof, where the organic inhibitor molecules replace the H_2O molecules on the metal roof [35] as observed in equation 12:

$$Org_{(sol)1} + nH_2O_{(ads)1} \leftrightarrow Org_{(ads)2} + nH_2O_{(sol)2} \ldots\ldots\ldots (12)$$

where the organic molecules of $Org_{(sol)1,}$ and $Org_{(ads)2,}$ represent the aqueous solution and the adsorbed solution on the steel roof, respectively, the $H_2O_{(ads)1}$ represents a H_2O molecule on the steel roof, and n represent the number of water molecules replaced by [35] one unit of SU.

Several parameters control the adsorption of the inhibitor on the metal surface, Physicochemical properties mainly effect the adsorption of these molecules [36, 37], which include the structure of electronic, the factor of steric, the density of electronic at donor site, functional groups, and the size of molecular which has the greatest effect [38]. According to the FTIR result, the starch-urea inhibitor contains oxygen atoms in its structure, each of which carry one or more pair of free electrons. As a result, the SU inhibitor is expected to adsorb on the metal surface due to the unoccupied d-orbitals with electrons of the metal atoms, which leads to covering a large surface area of mild steel. Cathodic restraints reduce least the reaction that occurs at the cathode, where the cathodic and anodic reactions correspond to OH^- and Fe^{2+}, respectively [39]:

$$Fe \rightarrow Fe^{2+} + 2e^{-}(anodic\ reaction) \ldots\ldots\ldots\ldots (13)$$

$$2H_2O + O_2 + 4e^{-} \rightarrow 4OH^{-}(cathodic\ reaction) \ldots\ldots\ldots (14)$$

The reaction of anodic inhibition on the surface of the metal is dominated by a figuration of a complex (Fe^{2+}−SU) on the metal surface anodic positions, whereas the cathodic inhibition reaction is controlled by a formation of an insoluble substance to form the hydroxide on the cathodic sites of the metal complex [39].

5. Conclusion

The corrosion of mild steel in 1M HCl with the presence and absence of SU blend as an inhibitor was investigated using the weight loss technique at a temperature range of 20–50∘C. The spectrum of FTIR shows clearly that natural polymer structure has C=O and O-H groups which lead to improving the adhesion of SU blend on iron metal surfaces. In comparison to the blank solution, the weight loss of mild steel minimizes at the inhibitor's loading into the acid solution. The rate of corrosion and inhibition efficiency were increased with increasing temperature. Maximum inhibitor efficiency was observed at concentration of 0.5 g/l of inhibitor and at temperature of 50°C. It has been suggested that the adsorption of starch/urea blend on the surface of mild steel follows a chemical adsorption. Adsorption isotherms of Temkin is the better fit of adsorption isotherms. In comparison to the blank solution, the activation energy and enthalpy of adsorption decrease in the presence of the SU blend. Adsorption entropy values in the negative range indicated an increase in system order.

References

[1] A. Sehmi, H. B. Ouici, A. Guendouzi, M. Ferhat, O. Benali, F. Boudjellal, *J. Electrochem. Soc.* **167**, 155508, (2020)

[2] S. Jayakumar, T. Nandakumar, M. Vadivel, C. Thinaharan, R. P. George, J. Philip, *J. Adhes. Sci. Technol.* **34**, 713, (2020)

[3] I. M. Alwaan, F. K. Mahdi, *Int. J. Chem. Eng.* **2016**, 1, (2016)

[4] J. A. Rodríguez, J. Cruz-Borbolla, P. A. Arizpe-Carreón, E. Gutiérrez, *Materials* **13**, 1, (2020)

[5] L. C. Murulana, M. M. Kabanda, E. E. Ebenso, *J. Mol. Liq.* **215**, 763, (**2016**)

[6] Z. El Adnani, M. Mcharfi, M. Sfaira, M. Benzakour, *Int. J. Electrochem. Sci.* **7**, 6738, (**2012**)

[7] K. Efil, I. B. Obot, *Met. Phys. Chem. Surfaces* **53**, 1139, (**2017**)

[8] Z. El Adnani, M. Mcharfi, M. Sfaira, M. Benzakour, A. T. Benjelloun, M. Ebn Touhami, *Corros. Sci.* **68**, 223, (2013)

[9] J. C. Valle-Quitana, G. F. Dominguez-Patiño, J. G. Gonzalez-Rodriguez, *International Scholarly Research Notices* **2014**, Article ID 945645, 8 pages (2014)

[10] N. Negm, M. Yousef, S. Tawfik, *Recent Patents Corros. Sci.* **3**, 58, (2013)

[11] X. Li, S. Deng, T. Lin, X. Xie, G. Du, *J. Mater. Res. Technol.* **9**, 2196, (2020)

[12] M. Mobin, M. A. Khan, M. Parveen, *J. Appl. Polym. Sci.* **121**, 1558, (**2011**)

[13] M. Manivannan, T. Nadu, S. Rajendran, T. Nadu, T. Nadu, *Int. J. Eng. Sci. Technol.* **3**, 8048, (2011)

[14] A. S. Abdullah, *Eng. sci. techn.: An internat. J.* **5**, 1, (2015)

[15] F. Bentiss, M. Traisnel, M. Lagrenee. *J. Appl. Electrochem.* **31**, 41, (2001)

[16] I. A. Akpan, N. A. O. Offiong, *Int. J. Corros.* **2013**, 1, (2013)

[17] X. Li, S. Deng, H. Fu, T. Li, *Electrochim. Acta* **54**, 4089, (2009)

[18] M. I. Khalil, S. Farag, K. M. Mostafa, A. Hebeish, *Starch - Stärke* **46**, 312, (1994)

[19] R. Santosh Kumar, K. P. R. Chowdary, *J. Drug Deliv. Ther.* **9**, 280, (2019)

[20] A. A. Khadom, *J. Chil. Chem. Soc.* **59**, 2545, (2014)

[21] R. Govindasamy, S. Ayappan, *J. Chil. Chem. Soc.* **60**, 2786, (2015)

[22] L. M. Rodríguez-Pineda, E. de J. Muñoz-Prieto, C. A. Rius-Alonso, J. Palacios-Alquisira, *Cienc. en Desarro.* **9**, 149, (2018)

[23] P. Siemion, J. Jabłońska, J. Kapuśniak, J. J. Kozioł, *J. Polym. Environ.* **12**, 247, (2004)

[24] Ime B Obot, Nelson Okpako Obi-Egbedi, S. Umoren, *J. Mater. Environ. Sci.* **2**, 60, (2011)

[25] N. Zulfareen, K. Kannan, T. Venugopal, S. Gnanavel, *Arab. J. Chem.* **9**, 121, (2016)

[26] M. Messali, H. Lgaz, R. Dassanayake, R. Salghi, S. Jodeh, N. Abid, O. Hamed, *J. Mol. Struct.* **1145**, 43, (2017)

[27] E. A. Noor, *Int. J. Electrochem. Sci.* **2**, 996, (2007)

[28] L. Tang, X. Li, Y. Si, G. Mu, G. Liu, *Mater. Chem. Phys.* **95**, 29, (2006)

[29] S. A. M. Refaey, F. Taha, A. M. A. El-Malak, *Appl. Surf. Sci.* **236**, 175, (2004)

[30] M. Jeeva, G. V. Prabhu, M. S. Boobalan, C. M. Rajesh, *J. Phys. Chem. C* **119**, 22025, (2015)

[31] N. B. Iroha O. Akaranta, *SN Appl. Sci.* **2**, 1514, (2020)

[32] A. Y. El-Etre, *Corros. Sci.* **45**, 2485, (2003)

[33] S. Bilgiç and M. Şahin, *Mater. Chem. Phys.* **70**, 290, (2001)

[34] N. Noorollahy Bastam, H. R. Hafizi Atabak, F. Atabaki, M. Radvar, S. Jahangiri, *Iran. J. Chem. Chem. Eng.* **39**, 113, (2020)

[35] S. Cheng, S. Chen, T. Liu, X. Chang, Y. Yin, *Mater. Lett.* **61**, 3276, (2007)

[36] D. M. Gurudatt, K. N. Mohana, H. C. Tandon, *Mater. Discov.* **2**, 24, (2015)

[37] M. Najafi Lahiji, A. R. Keshtkar, M. A. Moosavian, *Part. Sci. Technol. An Int. J.* **36**, 340, (2016)

[38] M. Yadav, D. Behera, S. Kumar, P. Yadav, *Chem. Eng. Commun.* **202**, 303, (2015)

[39] N. Saxena, S. Kumar, S. P. Mathur, *Chem. Eng. Commun.* **196**, 145, (2009)